

Negative Absorption near the Electron Cyclotron Harmonics in Weakly Ionized Gases

TOSHITAKA IDEHARA*, KATSUJI NAKAYA*
and YOSHIO ISHIDA*

(Received Apr. 15, 1969)

Negative absorption of radio frequency wave was observed near the electron cyclotron harmonics ($f=nf_c$) in weakly ionized plasma, and the voltage gains near $f=f_c$ and $f=2f_c$ were about 7dB and about 4dB, respectively. The emissions near $f=nf_c$ ascribed to this phenomenon were observed up to $n=4$ in Xe-plasma, up to $n=2$ in Kr-plasma and only at $n=1$ in Ar-plasma.

Their powers were stronger by several tens dB than that of thermal noise. Frequency shift from $f=nf_c$ as a function of the electron-neutral collision frequency was measured and compared with the theoretical result where the electron distribution function was assumed to be δ -functional.

1. Introduction

It was described by Twiss¹⁾ that negative absorption of the radio wave in a plasma are expected to occur when the Cerenkov effect, the cyclotron radiation or the synchrotron radiation is a dominant process. Since then, Bekefi et al.²⁾ and Tanaka et al.³⁾ discussed this phenomenon in detail and showed that the weakly ionized non-Maxwellian plasma with a large Ramsauer effect has a negative value for the absorption coefficient at the electron cyclotron frequency. Drummond et al.⁴⁾ and Shimomura et al.⁵⁾ solved the Boltzmann equation with a collision term and obtained the result that the instability can occur in the vicinity of $f=0$ (for longitudinal wave) and $f=f_c$ (for transverse wave) at the long wavelength limit when the electron distribution is δ -functional and collision frequency ν varies as $\nu \propto \nu^h$ with $h>3$.

Experimentally, one of the authors (T. I.) et al. and Tanaka et al. have shown⁶⁾⁷⁾ that amplification of rf wave occur for weakly ionized gases having large Ramsauer effect, in the vicinity of the electron cyclotron frequency ($f=f_c$) and low frequency region ($f/\nu \lesssim 1$) and it is interpreted as a negative absorption due to the stimulated cyclotron radiation and the stimulated bremsstrahlung, respectively.

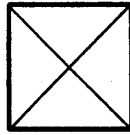
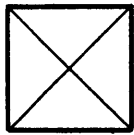
In this paper, it is described that amplification of rf wave also occur near the electron cyclotron harmonics ($f=nf_c$) in Xe and Kr plasmas and the frequency shift from $f=nf_c$ is observed when the collision frequency ν becomes large. The experimental apparatus and procedure are explained in §2, the experimental results are shown in §3 and these

* Dept. of Applied physics

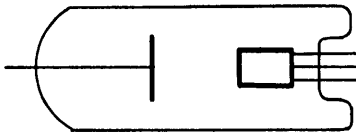
results are summarized and compared with the theoretical considerations in §4.

2. Experimental apparatus and procedure

Through the experiment, we used two discharge tubes; one (TUBE I) has a plane anode (20 mm in diameter) and an oxide-coated cathode (10 mm in diameter), their separation being 30 mm, and the other (TUBE II) has an anode (15 mm in diameter), a cathode (10 mm in diameter) and meshed grid, the separations between anode and cathode, and between grid and cathode being 33 mm and 3 mm, respectively. The



Helmholtz Coil



TEST TUBE

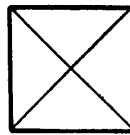
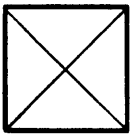
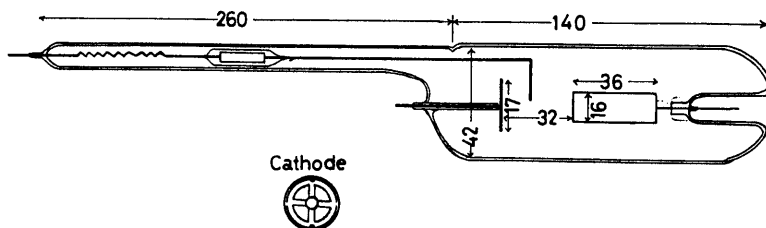


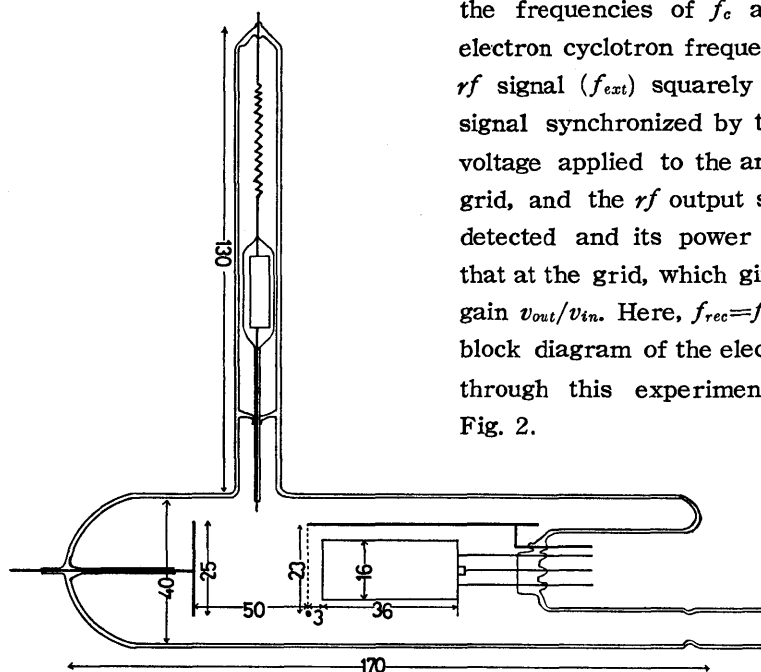
Fig. 1 (a) Schematic view of setting the test tube in the Helmholtz coil.

tubes are placed in the center of the Helmholtz coil and external magnetic field is applied parallel to the tube axes. The nonuniformity of the field $\Delta B/B$ is smaller than 3 percent through the region between the anode and the cathode, i.e., the plasma region. The plasma is produced by a dc discharge in a rare gas and often an external low frequency voltage is applied to the anode in order to modulate the dc discharge. Gas pressure is varied from 10^{-1} Torr to several Torr. Schematic view of the apparatus described above is shown in Fig. 1.

Each tube has a movable probe and electrical oscillations in plasma are picked up from this probe and amplified and detected by a field intensity meters, whose band widths (δf_{rec}) are about 0.5 MHz. Receiving frequency (f_{rec}) is varied from 90 MHz to 230 MHz. The output signal of the field intensity meter is traced on a XY-recorder as a function of the magnetic field intensity at fixed discharge current I_d , or is displayed on the synchroscope at fixed magnetic field and fixed discharge current. In the



(b) Sketch of the TUBE I.



(c) Sketch of the TUBE II.

3. Experimental results

3.1 Emission near the electron cyclotron harmonics

The emission from the plasma is observed by means of the apparatus, whose block diagram is shown in Fig. 2(a). The emission power from the plasma picked up by the probe is traced on a XY-recorder as a function of normalized external magnetic field intensity (f_c/f). An anomalous cyclotron emission ascribed to the negative absorption⁸⁾ is observed near the electron cyclotron frequency ($f=f_c$) in Xe, Kr and Ar plasma but not observed in Ne and He plasma. When a gas pressure p is adjusted at the suitable value ($p=0.10 \sim 0.25$ Torr), the anomalous harmonic emissions are also detected near the cyclotron harmonics ($f=nf_c$). In Fig. 3, are shown a typical emission spectrum as a function of an external magnetic field intensity (f_c/f). We have observed the anomalous harmonics up to the 4th in Xe plasma, up to the 2nd in Kr plasma but only at the fundamental in

experiment of amplification of rf wave at the frequencies of f_c and $2f_c$ (f_c is an electron cyclotron frequency), the external rf signal (f_{ext}) squarely modulated by lf signal synchronized by the low frequency voltage applied to the anode, is fed to the grid, and the rf output signal at anode is detected and its power is compared with that at the grid, which gives the rf voltage gain v_{out}/v_{in} . Here, $f_{rec}=f_{ext}=f_c$ or $2f_c$. The block diagram of the electrical circuit used through this experiment are shown in Fig. 2.

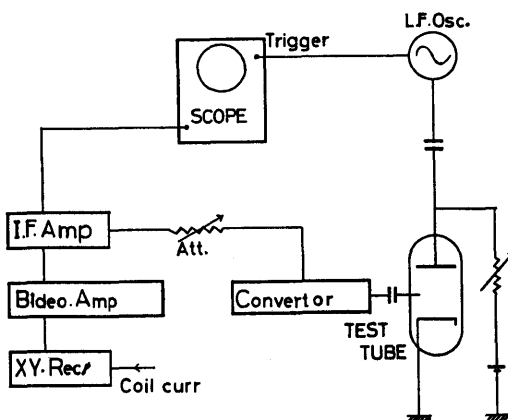
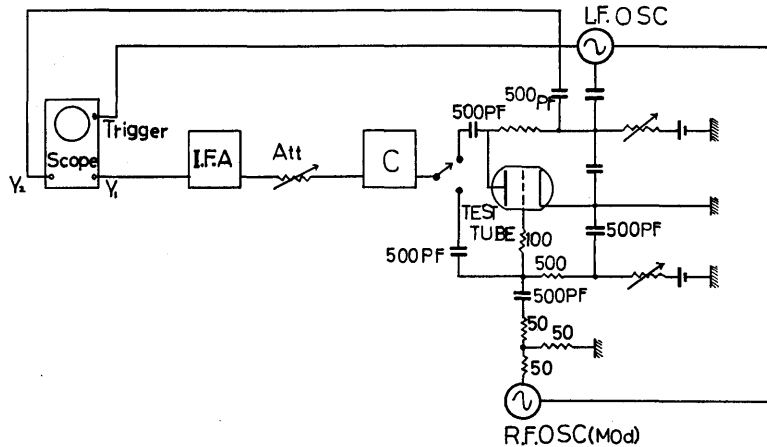
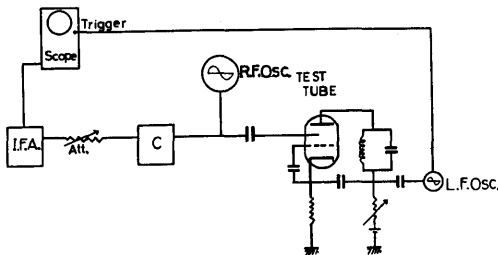


Fig. 2 (a) The block diagram of the experimental apparatus for the emission observation.



(b) The block diagram of the experimental apparatus for the observation of amplification.



(c) The block diagram of the experimental apparatus for the observation of self-oscillation.

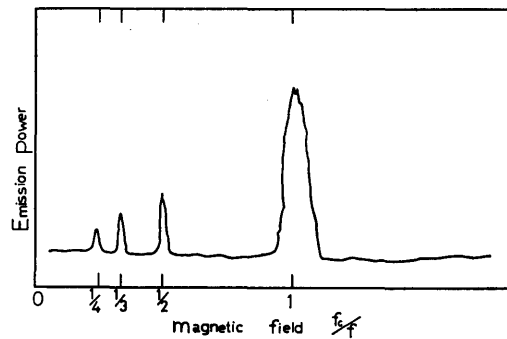


Fig. 3 Emission spectrum as a function of an external magnetic field intensity. Xe, $p=0.18$ Torr, $f=125$ MHz and $I_d=8$ mA.

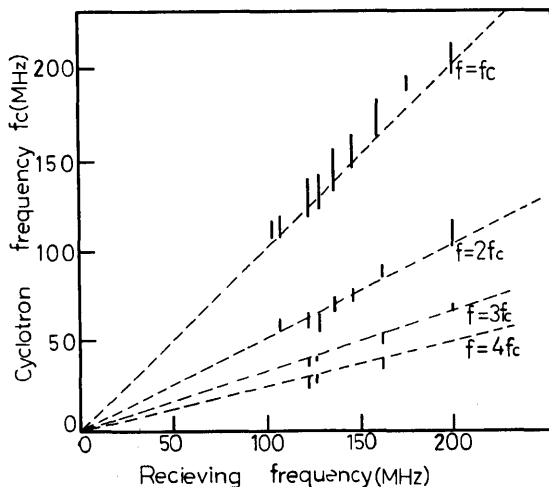
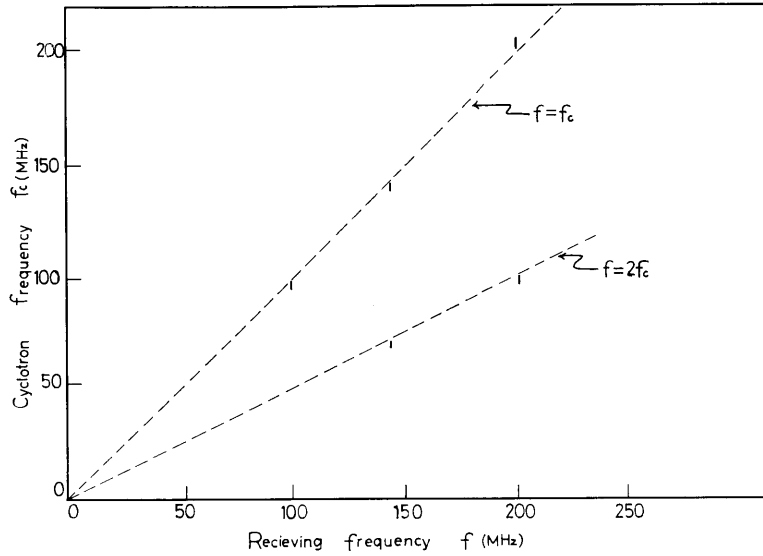
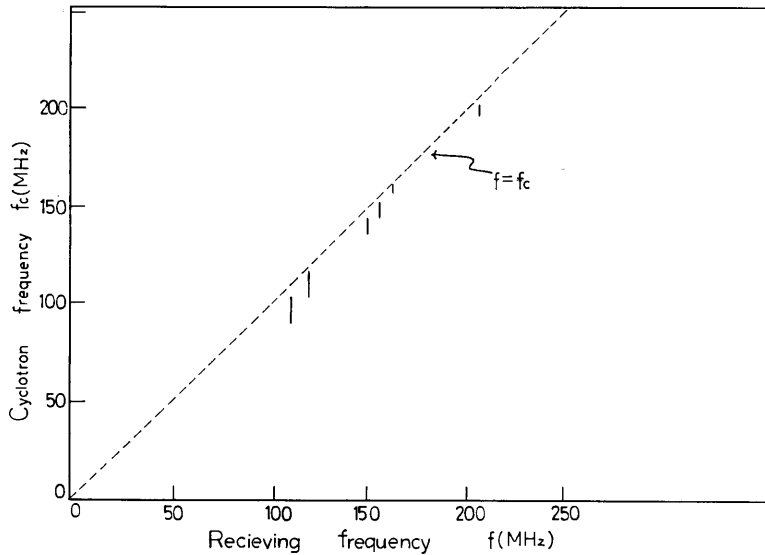


Fig. 4 The magnetic field f_c , where the emission is observed, as a function of receiving frequency.

(a) Xe, $p=0.18$ Torr and $I_d=8$ mA,

Ar plasma.

In Fig. 4, the magnetic field f_c , at which the anomalous harmonics are observed, is plotted as a function of the detecting frequency f , for the Xe, Kr and Ar plasma, respectively. The characteristics of these harmonics are similar to those of the anomalous cyclotron emission described in the other paper⁸⁾ as follows: 1) They are not stationary in time, but are pulsively emitted at a definite phase of low frequency oscillation existing spontaneously in dc discharge. 2) Their resonance lines are sharp and their widths

(b) Kr, $p=0.20$ Torr and $I_d=7.5$ mA.(c) Ar, $p=0.20$ Torr and $I_d=12$ mA.

are much narrower than those determined from the collision broadening. 3) The emission intensity is extremely larger than that of the black body, assuming that plasma electrons are in thermal equilibrium.

When an appropriate low frequency voltage is applied to the anode, the pulsed emission synchronizes with this voltage. Usually, the anomalous emissions at the fundamental ($f=93$ MHz) and at the 2nd harmonic ($f=186$ MHz) are both observed at the same time, as shown in Photo. 1(a). However, if the applied low frequency voltage appropriately modulates the *dc* discharge, they do not occur at the same time (Photo. 1(b)).

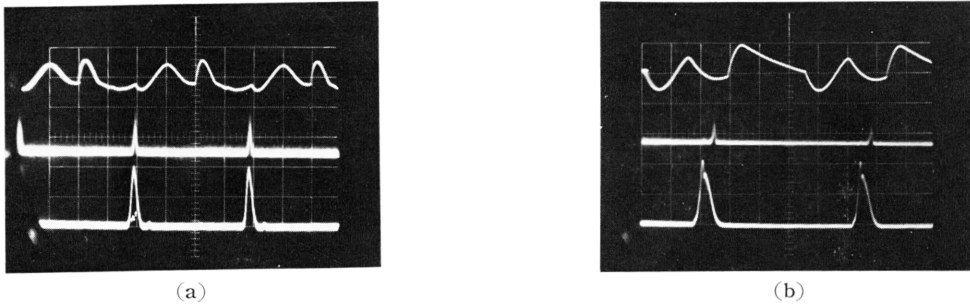


Photo. 1 The anomalous emissions. Upper trace: low frequency signal at the anode. Middle trace: emission power at the cyclotron frequency. $f=f_c=93\text{ MHz}$. Lower trace: emission power at the second harmonic. $f=2f_c=186\text{ MHz}$. $200\mu\text{ sec/div}$.
 (a) Xe, $p=0.21\text{ Torr}$ and $I_d=7.5\text{ mA}$.
 (b) Xe, $p=0.18\text{ Torr}$ and $I_d=7.0\text{ mA}$.

3.2 Amplification of the radio wave near the 2nd harmonic

The amplification of rf wave is observed by using the apparatus as shown in Fig. 2 (b). An appropriate external low frequency voltage is applied to the anode in order to modulate the dc discharge and such a plasma that amplifies rf wave is produced. Measurements are carried out by a field intensity meter at a fixed frequency of $f=93\text{ MHz}$ or 186 MHz . The external rf signal (f_{ext}) squarley modulated by lf signal, is fed to the grid and the rf output signal at the anode is detected. The lower trace in Photo. 2 (a) and (b) show respectively the input signal at grid and the output signal at anode. Here, the cyclotron frequency of the external magnetic field is set at $f_c=93\text{ MHz}$ and the frequency of rf signal is adjusted to be twice f_c , i.e., $f=f_{ext}=2f_c=186\text{ MHz}$.

The upper traces show the anode potential modulated by lf voltage. Comparing the output signal (v_{out}) with the input signal (v_{in}), it is known that the input signal is amplified at a certain phase of lf voltage φ_1 . The rf voltage gain is about 4 dB . Since the ratio of the input impedance to the output one is estimated to be 3 dB from Fig. 2 (b), the

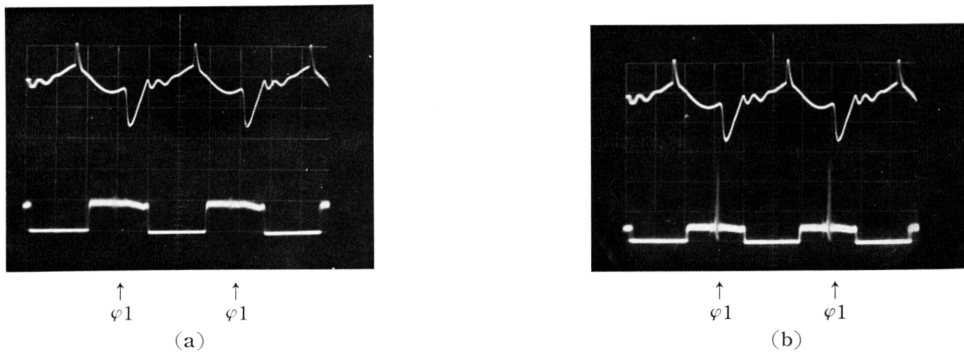


Photo. 2 (a) Upper trace: low frequency signal at the anode. Lower trace: rf input signal at the grid.
 (b) Upper trace: low frequency signal at the anode. Lower trace: rf output signal at the anode.
 Xe, $p=0.47\text{ Torr}$, $f=f_{ext}=186\text{ MHz}$, $f_c=93\text{ MHz}$, $I_d=3.6\text{ mA}$ and sweep: $200\mu\text{ sec/div}$.

power gain is about 7 dB. Measurements at the receiving frequency of 93 MHz show that the amplification occurs also at the fundamental frequency ($f=f_{ext}=f_c=93$ MHz), by about 9 dB.

Fig. 5 shows the voltage gain as a function of rf input power both at the cyclotron frequency and its 2nd harmonic. Usually, the input power, where the amplification occurs at the 2nd harmonic, is smaller than that at the fundamental. Exceeding a certain value of input power, the voltage gain decreases with increasing input power, and a saturation effect is expected as seen in Fig. 5.

3.3 Observation of the self-oscillation near $f=nf_c$

As shown in Fig. 2 (c), the rf signal from the anode is fed back to the grid in order to make the self-oscillation at the resonant frequency. Near the fundamental frequency ($f=f_c$) and the 2nd harmonic ($f=2f_c$), when the value of capacity of the external circuit is adjusted at the appropriate value, the rf oscillation occurs strongly. In Photo. 3 (a), is shown the rf signal from the probe at the fundamental frequency. In Photo. 4, are shown the direct observation of rf signal in the case of particularly large one, by means of 100 MHz synchroscope, which shows that the oscillation is sinusoidal and its peak-to-peak-voltage is about 0.04 mV. When the external signal whose frequency is near the receiving frequency ($f_{ext} \approx$), the beat of the both signals,

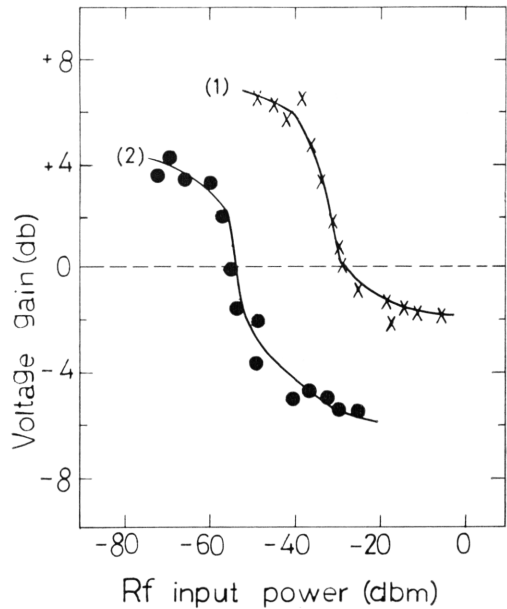
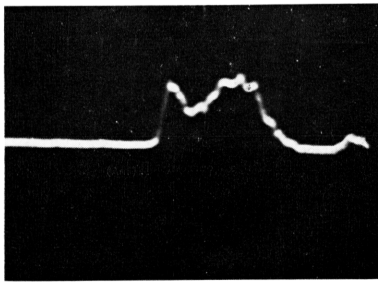
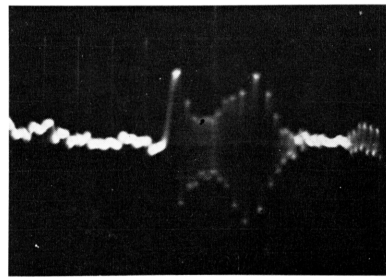


Fig. 5 The voltage gain as a function of rf input power at the cyclotron frequency and its second harmonic.

- (1) for the cyclotron frequency, $f_{rec}=f_{ext}=f_c=93$ MHz.
- (2) for the second harmonic, $f_{rec}=f_{ext}=2f_c=186$ MHz.



(a)



(b)

Photo. 3 (a) Anomalous emission pulse.

(b) Beat of an anomalous emission with an external signal.

Xe, $p=0.27$ Torr, $I_d=4.2$ mA, $f=f_c=93$ MHz and sweep: 100μ sec/div.

i.e., the external signal and the oscillation signal in a plasma-external-circuit system, are observed as shown in Photo. 3 (b). From this photograph, it is confirmed that the oscillation is coherent but the frequency is varied in a single pulse. The variation of frequency δf seen in this photograph is about 140 KHz and comparable with the band width δf_{rec} of a field intensity meter used here. This value of δf is often larger than that of δf_{rec} and reach several MHz.

3.4 Frequency shift from $f=nf_c$ as a function of background pressure p

Fig. 6 shows the emission spectrum as a function of the magnetic field intensity (f_c/f) with I_d as a parameter. It is seen from this figure that the value of the magnetic field intensity where the emission is observed is shifted with increasing I_d . This frequency shift ($\Delta f_c/f$) can not be interpreted as the nonuniformity of the external magnetic field ($\Delta B/B$) through the plasma region, because $\Delta f_c/f$ is about ten percent and much larger than $\Delta B/B$ (~ 3 percent). The magnetic field intensity f_c/f where the emission is observed is plotted as a function of I_d in Fig. 7. From this figure, the maximum value of this shift ($\Delta f_c/f$)_{max} are determined for the certain value of back ground pressure p . By measuring for the various values of p , it is known that ($\Delta f_c/f$)_{max} varies as a function of p , as shown in Fig. 8.

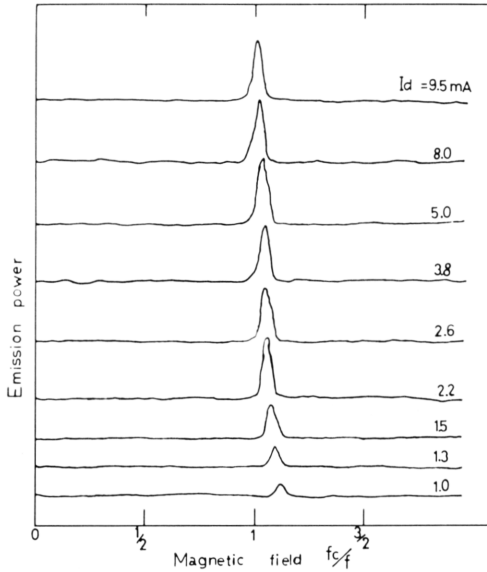


Fig. 6 Emission spectrum as a function of the magnetic field intensity with I_d as a parameter. Xe, $p=0.75$ Torr and $f=150$ MHz.

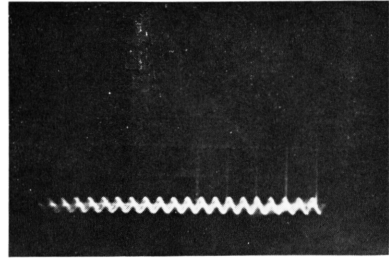


Photo. 4 Direct observation of the oscillation due to the negative absorption at the cyclotron frequency. sweep: 0.05μ sec/div.

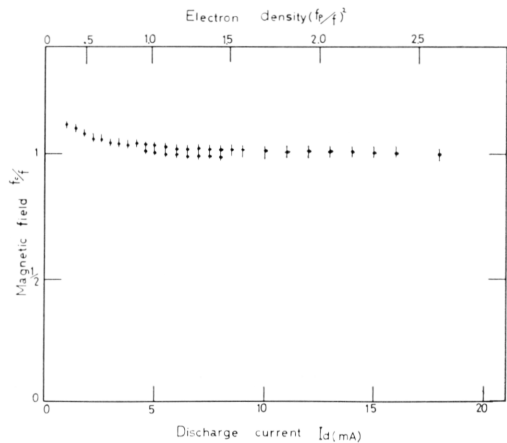


Fig. 7 The magnetic field intensity f_c/f , where the emission is observed, as a function of I_d . Xe, $p=0.75$ Torr and $f=150$ MHz.

4. Discussion

The experimental results described in §3 are summarized as follows :

- I) Negative absorption phenomenon due to the Ramsauer effect occurs not only near the cyclotron frequency but also near its 2nd harmonic. The anomalous emission ascribed to this phenomenon is observed at the higher harmonics up to 4th.
- II) The system composed from the plasma and external circuit self-oscillates pulsively at the cyclotron frequency and its 2nd harmonic, but the frequency shift ($\delta f \sim$ several MHz) is observed in a single pulse.
- III) The frequency at which the anomalous emission is observed shifts with increasing I_d and the maximum value of this shift $(\Delta f/f)_{max}$ increases with a background pressure p .

On the other hand, the possibility of the negative absorption near the cyclotron harmonics is discussed theoretically elsewhere⁹⁾. Following them, the assumptions are as follows :

- 1) The zeroth order distribution function is δ -functional;

$$f_0 = \frac{1}{4\pi v_o^2} \delta(v - v_o). \quad \dots\dots\dots(1)$$

- 2) The collision frequency of an electron with neutral atoms is proportional to v^h ;

$$\nu \propto v^h. \quad \dots\dots\dots(2)$$

- 3) The collision term of the Boltzmann equation is assumed as follows;

$$\left(\frac{\partial f}{\partial t} \right)_{coll} = -\nu(v) f(r, v, t) + \frac{1}{4\pi} \int \nu(v) f(r, v, t) d\Omega, \quad \dots\dots\dots(3)$$

where $d\Omega$ is the elementary solid angle in velocity space.

By solving the Boltzmann equation under these assumptions, the dispersion relation for the extraordinary wave near the cyclotron harmonics ($f \approx nf_c$) with $k^2 c^2 / \omega^2 \gg 1$ is as follows;

$$\omega(\omega - n\omega_c + i\nu)^2 = \frac{n^2}{(2n)!} \omega_p^2 \lambda_o^{2n-2} (\omega - n\omega_c + i \frac{2n+1-h}{2n+1} \nu_o), \quad \dots\dots\dots(4)$$

where $\omega = 2\pi f$, k is a propagation constant, $\lambda_o = kv_o / \omega_c$ and $\nu_o = \nu(v_o)$. It is confirmed from this equation, that the negative absorption occur near the n th cyclotron harmonics, for the extraordinary wave if h is larger than $2n+1$. Under the same assumptions as mentioned above, the negative absorption for the ordinary wave with $k^2 c^2 / \omega^2 \gg 1$ is exp-

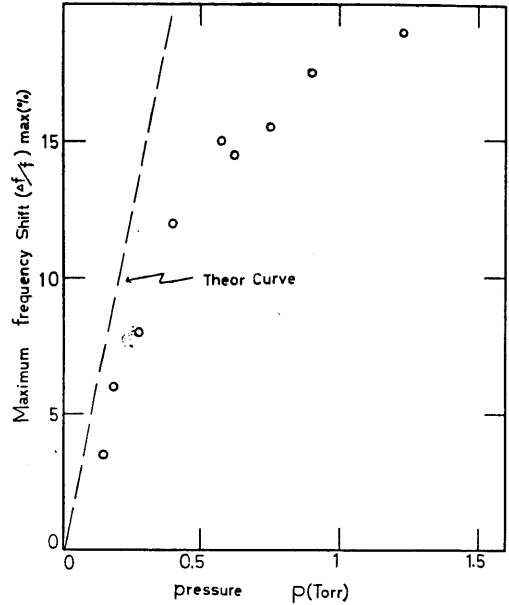


Fig. 8 Maximum frequency shift as a function of pressure. Theoretical curve is drawn by using Eq. (5) and substituting the experimental conditions to it.

ected to occur near the n th harmonics if h is larger than $2n+3$.

We will compare this theoretical consideration with the experimental results in order to give them the qualitative interpretation, though it is combined with the severe assumptions.

- 1) The wavelength is considered to be comparable with the plasma scale and the condition of $k^2 c^2 / \omega^2 \gg 1$ is satisfied for our plasma.
- 2) The observed wave do not propagate perpendicularly to the magnetic field. However, as k has a component perpendicular to the magnetic field, it is expected that the theory mentioned above is fitted to our experiment qualitatively.
- 3) The assumption of $\nu \propto \nu^h$ describes the Ramsauer effect expected in our plasma.
- 4) The assumption that the distribution function is a δ -functional, describes the population inversion expected in our plasma, qualitatively.
- 5) In Xe plasma whose value of h is considered to be largest among rare gases, the highest order harmonics is observed.

This is consistent with the theoretical results.

- 6) In Fig. 9, are plotted the dispersion curve from Eq. (4). This curve shows that the magnetic field where the negative absorption occurs, shifts with the plasma density. This interpretes the experimental results shown in Fig. 7, qualitatively.
- 7) From Eq. (4), the maximum frequency shift $(\Delta f/f)_{max}$ is calculated as follows ;

$$(\Delta f/f)_{max} \approx 0.30 \frac{h}{2n+1} \frac{\nu}{f} \quad \dots\dots\dots(5)$$

This curve is plotted in Fig. 8 and its tendency is consistent with the experimental one.

From the reasons mentioned above, the theory interpretes the experimental results qualitatively. After all, we want to emphasize through the paper that the negative absorption occur not only near the electron cyclotron frequency but also near the cyclotron harmonics.

Acknowledgement

The authors wish to express their sincere thanks to Professor S. Tanaka and Dr. Y. Terumichi of Kyoto University for their valuable discussions.

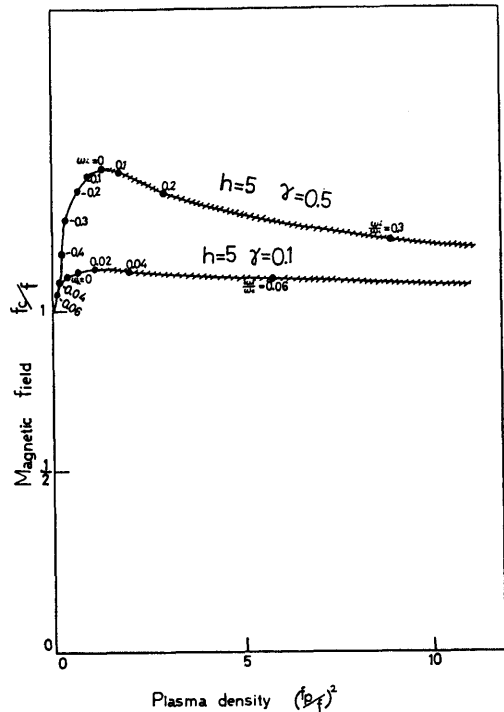


Fig. 9 Dispersion curves with $\gamma (= \nu_0/\omega_r)$ as a parameter. Imaginary part of the frequency (ω_i/ω_r) is shown on these curves. In the hatched region, where ω_i/ω_c is positive, the negative absorption is expected to occur.

References

- 1) R. Q. Twiss : Australian J. Phys. **11** (1956) 564.
- 2) G. Bekefi, J. L. Hirshfield and S. C. Brown : Phys. Fluids **4** (1961) 173.
- 3) S. Tanaka and K. Mitani : J. Phys. Soc. Japan **19** (1964) 1376.
- 4) J. E. Drummond, D. J. Nelson and J. L. Hirshfield : to be published.
- 5) N. Shimomura, K. Mitani and S. Tanaka : J. Phys. Soc. Japan **21** (1966) 1372.
- 6) Y. Terumichi, T. Idehara, I. Takahashi, H. Kubo and K. Mitani : J. Phys. Soc. Japan **20** (1965) 1705.
- 7) S. Tanaka and K. Takayama : J. Phys. Soc. Japan **22** (1967) 310.
- 8) For example, this is reported by S. Tanaka et al. in J. Phys. Soc. Japan **18** (1963) 1810.
- 9) T. Idehara and R. Sugaya : J. Phys. Soc. Japan **23** (1967) 1122.